# INFILL LOCATION DETERMINATION AND ASSESSMENT OF CORRESPONDING UNCERTAINTY

A Thesis

by

OZGUR SENEL

Submitted to the Office of Graduate Studies of
Texas A&M University
in partial fulfillment of the requirements for the degree of

MASTER OF SCIENCE

May 2008

Major Subject: Petroleum Engineering

# INFILL LOCATION DETERMINATION AND ASSESSMENT OF CORRESPONDING UNCERTAINTY

A Thesis

by

OZGUR SENEL

Submitted to the Office of Graduate Studies of
Texas A&M University
in partial fulfillment of the requirements for the degree of

MASTER OF SCIENCE

Approved by:

Chair of Committee, Duane A. McVay
Committee Members, W. John Lee
J. Eric Bickel
Head of Department, Stephen A. Holditch

May 2008

Major Subject: Petroleum Engineering

# ABSTRACT

Infill Location Determination and Assessment of Corresponding Uncertainty.

(May 2008)

Ozgur Senel, B.Sc., Middle East Technical University

Chair of Advisory Committee: Dr. Duane A. McVay

Accurate prediction of infill well production is crucial since the expected amount of incremental production is used in the decision-making process to choose the best infill locations. Making a good decision requires taking into account all possible outcomes and so it is necessary to quantify the uncertainty in forecasts. Many researchers have addressed the infill well location selection problem previously. Some of them used optimization algorithms, others presented empirical methods and some of them tried to solve this problem with statistical approaches. In this study, a reservoir simulation based approach was used to select infill well locations. I used multiple reservoir realizations to take different possible outcomes into consideration, generated probabilistic distributions of incremental field production and, finally, used descriptive statistical analysis to evaluate results. I quantified the uncertainty associated with infill location selection in terms of incremental field production and validated the approach on a synthetic reservoir model. Results of this work gave us the possible infill locations, which have a mean higher than the minimum economic limit, with a range of expected incremental production.

# ACKNOWLEDGEMENTS

I would like to thank my parents for their constant support, my brothers for their encouragement and Dr. McVay for his patience and assistance. I would like to dedicate this work to my lovely grandmother for her prayers.

TABLE OF CONTENTS

Page

# LIST OF TABLES

# LIST OF FIGURES

FIGURE Page

# INTRODUCTION

Reservoir management is not simply the creation of a depletion plan and/or a development plan but rather a comprehensive, integrated strategy for reservoir exploitation.[1] Infill location determination and maximizing corresponding incremental field production are critical aspects of optimal reservoir management. Estimating infill development potential and forecasting incremental reserves are challenging problems in mature tight gas fields due to lack of static and dynamic data, large variability in rock quality, well spacing, and the large number of wells involved. Accurate prediction of infill well production is crucial since the expected amount of incremental production is used in the decision-making process to choose the best infill locations.

Making a good decision requires taking into account all possible outcomes and so it is necessary to quantify the uncertainty in forecasts[2]. In other words, if there is no uncertainty quantification in the decision-making process or the uncertainty quantification is incomplete, then the decision may be poor. Thirty years ago Capen[3] showed that people in the oil industry significantly underestimate uncertainty in their assessments and, recently, Floris *et al.*[4] showed that, even when we try to quantify uncertainty in simulation studies explicitly, we still tend to underestimate it. Similarly, engineers continue to take only limited consideration of uncertainty and most of the time do not try to quantify it at all. Reservoir simulation techniques play a vital role in reservoir management and can be used to quantify uncertainty. Reservoir models

---

This thesis follows the style of *SPE Reservoir Evaluation & Engineering.*

conditioned to historical data can be used to predict future responses of the reservoir as well as to select infill locations. Although it is not literally possible to find and use all possible combinations of reservoir parameters, uncertainty in forecasts can still be quantified and used in the decision-making process.

This thesis investigates uncertainty quantification in infill well location selection using multiple reservoir realizations. The process is described in detail below. The proposed method was applied on a synthetic reservoir with an actual gas field's production data.

## HISTORY AND CURRENT STATUS

In the past decade, various approaches have been proposed for selection of infill locations. Those approaches can be classified in two categories; empirical/statistical analyses and numerical simulation coupled with optimization algorithms.

Thirty years ago Capen[3] demonstrated that the oil industry significantly underestimates uncertainty in its assessments. However, the oil industry is making a great effort to improve uncertainty assessments. Beckner and Song[5] applied the traveling salesman framework on a well placement problem using simulated annealing (SA) to find the optimum locations of the wells. Farnstrom and Litvak[6] developed a deterministic method that automates simulation to estimate infill development potential and forecast incremental reserves of Prudhoe Bay Field. McCain *et al.*[7] and Voneiff and Cipaolla[8] used a statistical-moving window method to select infill locations. However, Guan *et al*.[9] indicated that accuracy of predictions for individual wells can be off by more than 50%. Badru and Kamir[10] coupled Genetic Algorithms with a polytype algorithm and reservoir simulation for gas and water injection projects to optimize the number of wells and well locations. However, they used a single reservoir realization, ignoring the uncertainty in reservoir parameters. Gao and McVay[11] focused on large-scale, moderate-resolution problems and presented a simulation-based inversion approach for rapid assessment of infill well potential. They used the inversion method for history matching, and used a single realization for prediction and infill well selection. They made a forecast run with existing wells and placed an infill well in each grid block

sequentially and estimated incremental field production. At the end of this process, they chose the location with maximum incremental field production. However, they did not address the interference problem between new infill wells.

Cheng *et al.*[12,13] upgraded simulation-based inversion approach and developed a deterministic method that addresses the well interference problem including the interference between the new infill wells. After selecting the location of the first infill with the method developed by Gao and McVay[11], they discarded the grid cell which have incremental production value lower than the minimum limit and did not consider them for further evaluation as candidate location. Assuming that the first infill candidate will be drilled and produced, authors placed another infill well sequentially in each grid cell within the boundaries of an influence area around this well and ran the forecast simulations. After running the procedure, values of the incremental field production are updated for each cell in the influence region. A new field-wide distribution is obtained by updating the incremental field production values. The grid cell with the highest value in this field-wide distribution is the location for the second optimal infill well. Similarly, a new influence region is evaluated around the second infill well and the process is repeated until the last economical infill well is found. This process properly accounts for interference effects between the infill wells.[12]

Guyaguler *et al.*[14] proposed a deterministic multiplacement method for infill location determination. The multiplacement approach ignores the interference effects between the wells. In this approach, location selection for all wells is performed simultaneously ignoring the dynamic effects of previously drilled infill wells on

reservoir performance. However, as Cheng *et al.*[13] addressed, the new production data gathered from each new infill should be considered to update reservoir simulation model for more accurate and effective well placement.

Allard *et al.*[15] proposed an empirical method which uses offset producer liquid-rate and water-cut to select infill locations in the Barrow Island Field. Moreover, they used a probabilistic approach to include risk and uncertainty in the decision-making process. Although the accuracy of the results did not satisfy them, they concluded that the probabilistic method gives more reliable results than the deterministic method. It is well understood in the oil industry that a probabilistic answer to an uncertain problem is more helpful and valuable than a deterministic one in the decision-making process.

Numerical simulation is often the most appropriate tool to evaluate the feasibility of well configurations.[9,11,13,16,17] However, the data used to establish numerical models have uncertainty, as do the model forecasts. The uncertainties in the model are reflected in the uncertainties of the outcomes of well-placement decisions.[17] All the studies mentioned above looked for a better method to select infill locations. The main purpose of the studies was to choose the best combination of infill well locations. For this purpose different algorithms were coupled with reservoir simulators to reduce the time and cost; however, most of them presented a deterministic answer to a highly uncertain problem[6-12,14,16]. In other case[17], although they presented probabilistic solutions, because of the logic behind the optimization processes, instead of searching for all possible locations in the reservoir, limited numbers of locations were evaluated to reduce the amount of simulation time and minimize the cost. The performance of a

reservoir depends on static reservoir properties and also on time and process.[10] Guan *et al.*[9] claimed that the most accurate way to determine infill potential is to conduct a complete reservoir evaluation involving geological, geophysical, and reservoir analyses. These include geological model development, static reservoir properties' estimation, and reservoir simulation model construction and calibration to predict future outcomes. People in oil industry aware of the uncertainty associated with static and dynamic variables affecting reservoir performance. This uncertainty, in turn affects infill location determination. Hence, no single realization is completely representative of the reservoir.[10] Rather than the most likely value, the decision maker must account for all possible outcomes and then associated probabilities to make a better decision. Although it is not possible to sample all possible outcomes of a certain event, with current technology a reasonable and manageable number of realizations can be created for the purpose of quantifying uncertainty in predicted infill well performance.

The objective of this research is to present a simulation-based probabilistic solution to infill location selection problem searching the complete area of the reservoir, defining all the economical locations.

# METHODOLOGY

## Overview

In this research I used a method similar to the one proposed by Cheng *et al.*[13] However, rather than a deterministic approach, I used a probabilistic approach to quantify associated uncertainty in infill location determination.

Conducting a reservoir simulation study for probabilistic infill well location selection requires the combination of several components. First, multiple geostatistical reservoir realizations must be created and conditioned to the available historical data. Since I used multiple realizations, a code was developed to run the history matching process and evaluate the results automatically. Next, after creating history-matched realizations, those models were used to predict reservoir performance. An infill well was located in each grid-block sequentially and reservoir performance was predicted. After repeating this process for multiple realizations, for each grid cell I obtained a probabilistic distribution of incremental field production due to a well located in that cell. Finally, statistical analyses were conducted to choose optimum locations for infill wells. For the performance prediction I used the commercial reservoir simulator Eclipse. I developed a Visual Basic code that automates the simulation runs and reduces human interaction. Below, I will describe the implementation of each of these elements in this study.

History Matching Using Sequential Inversion Method

Before we can start making prediction simulation runs, it is necessary to prepare history matched realizations of the reservoir. In this work, I used the sequential inversion method presented by Cheng *et al.*[13] Prior to history matching, I created a number of geostatistical reservoir models for the sequential inversion method considering the available porosity and permeability data.

The sequential inversion method employs well locations, production data and an approximate reservoir description. A reservoir simulator serves as the forward model and calculates well production responses from reservoir description data. This method uses a conventional 2D, single-phase, finite-difference gas reservoir simulator as a forward model to calculate reservoir and well performance. Sensitivity coefficients are calculated internally and used in the inversion of historical data to estimate the permeability and porosity fields. Since we rely primarily upon available well location and production data, wells are produced in the simulation at estimated flowing bottomhole pressure and match on production data, rather than producing at historical rates and matching on pressure.

This method consists of two components: forward and inverse modeling. During the forward modeling, simulator computes individual well and cumulative field production responses based on a prior geological model and other available reservoir data. Inverse modeling uses generalized pulse-spectrum technique (GPST) for sensitivity calculation and consists of automatic history matching process that adjusts porosity and permeability until the best fit of calculated response to historical production is achieved.

The sensitivity is obtained by partially differentiating the governing flow equation with respect to permeability or porosity. Since production data used for history matching are available only at grid blocks with wells and only at time steps after wells are put into production, the calculation of sensitivity coefficients is conducted to include the grid blocks with wells on production.

In sequential inversion approach with generalized pulse-spectrum technique there are two sets of inverse parameters considered: permeability and a multiplier that is applied to the initial pore volume distribution, so the parameter that is being inverted is effectively pore volume. The sequential inversion method proposed by Cheng *et al.*[13] can be briefly described as follows:

- Run the forward model and calculate sensitivity coefficients of production response with respect to permeability using GPST.
- Conduct inverse modeling to estimate the change in permeability required to honor the production data, and update the permeability field correspondingly.
- Run the forward model with the calibrated permeability field and calculate sensitivity coefficients of production response with respect to pore volume using GPST.
- Conduct inverse modeling to estimate the change in pore volume required to honor the production data, and update the pore volume field correspondingly.
- Iterate between inversion on permeability and pore volume until convergence.

Derivation of the sensitivity coefficients of production rate with respect to permeabilities can be described as follows.

The simplified governing equation can be written in the following form,

$$Ap = b \quad \text{.....(1)}$$

In this equation *A* is the matrix of flow elements, *p* is the vector of well block pressures, and *b* is comprised of the known pressures. Taking the partial derivative of Eq. 1 with respect to the *i-th* grid block permeability and simplifying, the following equation is obtained.

$$\frac{\partial p}{\partial k_i} = A^{-1}\left(\frac{\partial b}{\partial k_i} - \frac{\partial A}{\partial k_i}\, p\right) \quad \text{.....(2)}$$

Taking the partial derivative of Peaceman's equation,

$$q = J\left(p - p_{wf}\right) \quad \text{.....(3)}$$

with respect to the i-th grid block permeability, the following equation is obtained.

$$\frac{\partial q}{\partial k_i} = \frac{\partial J}{\partial k_i}\left(p - p_{wf}\right) + J\,\frac{\partial p}{\partial k_i} \quad \text{.....(4)}$$

Sensitivity coefficients of production data in all the grid blocks to one permeability value, $k_{i,}$ is obtained substituting Eq. 2 into Eq. 4.

$$\frac{\partial q}{\partial k_i} = \frac{\partial J}{\partial k_i}\left(p - p_{wf}\right) + JA^{-1}\left(\frac{\partial b}{\partial k_i} - \frac{\partial A}{\partial k_i}\, p\right) \quad \text{.....(5)}$$

Rather than calculating the inverse matrix of *A*, only the rows corresponding to the well blocks are calculated since we need sensitivity coefficients in the grid blocks with wells.[11]

## Field Performance Prediction

I used the Eclipse black oil simulator together with the calibrated reservoir models for prediction runs. I developed a Visual Basic code that automates the simulation runs and reduces human interaction. This code changes the reservoir property files which include porosity and permeability data for the simulator for each realization. For a particular realization, it updates the schedule file to define the location and production program for the infill well. It launches the simulation and at the end of each simulation it stores the output files for incremental field production evaluation. Since I use multiple reservoir models for prediction purposes, when we are simulating the historical part it is possible to obtain different cumulative production values at the end of history. To eliminate the effect of different cumulative production values for different realizations I used incremental field production to evaluate the infill location selection.

For each realization, a base case forecast run was made with the existing wells. For all cases in this research I used an economic life of 20 years with no abandonment cost. In a single run, a new well was placed in each grid block which does not have an existing well and a forecast run was made to estimate incremental field production considering the interference effects between existing wells and the infill well. After repeating this process for every grid block, I obtained an incremental field production value due to the placement of an infill well in that grid block. After repeating this process for multiple realizations, for each grid cell we obtained distribution of incremental field production values.

Discounted Incremental Field Production Evaluation

Rather than evaluating infill well's performance, field performance was evaluated to consider the well interference effects. In order to evaluate simulation results, I created a code that can handle large amounts of data. This code reads the simulation results from text files and stores the forecasted production values at discrete points, specifically the $2^{nd}$, $5^{th}$, $10^{th}$, $15^{th}$ and $20^{th}$ years, in a spread sheet.

In order to calculate incremental field production, difference between infill case production and base case production between the discrete points was calculated. For instance, for a given realization, after running the base case, an infill well was located on the first grid block and another prediction run was made. After the prediction run, production amount between the discrete points was calculated for the infill case and the base case. Once we obtained the production difference between the discrete points, we calculated the incremental amount, subtracting the base case production from the infill case production. Next, incremental field production was discounted to time zero using the midpoint between the discrete points; e.g., the difference in base case and infill case production between the $15^{th}$ and $20^{th}$ years was discounted for 17.5 years. In this work a discount rate of 8% was assumed. After discounting and summing the production amounts between the discrete points, discounted incremental field production was obtained for each grid block. This process was repeated until each realization is used for prediction. After all realizations are used, each grid cell has a distribution of discounted incremental field production due to an infill well located in that cell.

## Uncertainty Assessment

The final step in this process is comparing the discounted incremental field production values for each grid block. Descriptive statistical analyses were used to evaluate incremental field production distributions. A visual basic code was generated to calculate minimum, maximum, mean, standard-deviation, P10, P50, and P90 values of the distributions. In this study our discussion focused on the characteristics of the means and standard deviations of the distributions. A cross-plot of means and standard deviations was used to select the best candidates.

## Summary

Infill location determination and assessment of corresponding uncertainty is a multi-step process. First, multiple realizations of the reservoir are created. Next, reservoir models are calibrated with a sequential inversion method. Then the calibrated models are used to predict reservoir performance with an infill well. Next, discounted incremental field production is calculated. Finally, the results of individual runs are combined into probabilistic forecasts for each grid cell.

# SYNTHETIC RESERVOIR STUDY

## Overview

I applied this method on a synthetic case which is used by Holmes *et al.*[2]. The synthetic model was derived from a subsection of a multilayer-tight gas field **Fig. 1**. Though it is not a traditional clearly delineated reservoir, the edge of the reservoir was treated as a no-flow boundary. There are 40 wells in the reservoir, 38 which are still producing. The wells were drilled at different dates over the reservoir's life, represent its several rounds of infill drilling, **Table 1**.

The synthetic model represents a mature study area that first began producing 60 years ago. It was initially developed on 640-acre spacing. Later, well spacing was reduced to 320-acre and then 160-acre spacing. Presently, 80-acre infill wells are being drilled in some parts of the field. Cumulative production for the study area is shown in **Fig. 2**. We can see that the study area has produced approximately 73 million Mscf of gas during its productive life.

The synthetic reservoir representing a 9-township area was modeled using a 2304-cell single-phase Eclipse simulation model. This model is a single-layer, 48-by-48 grid. A geostatistical tool was used to generate base permeability fields. A log-normal distribution with a mean of 0.3 md and a standard deviation of 0.15 md was used as the prior distribution for permeability. Use of a geostatistical tool prevented extreme and unrealistic values of permeability. I generated 150 base permeability fields were in total.

**Figs. 3** and **4** show the prior probability density and cumulative distribution functions of permeability.

Permeability fields were converted into porosity fields using a power law equation;

$$\phi = a + b \log k \quad \text{.....(6)}$$

Maximum and minimum values for porosity were selected and used to calculate the values of coefficients in the power law equation. Maximum and minimum values of porosity and permeability and corresponding coefficient values are listed in **Table 2**. After calculating the power law equation's coefficients, base porosity fields were created using corresponding base permeability fields. Probability density and cumulative density functions of the porosity distribution can be seen in **Figs. 5 and 6**.

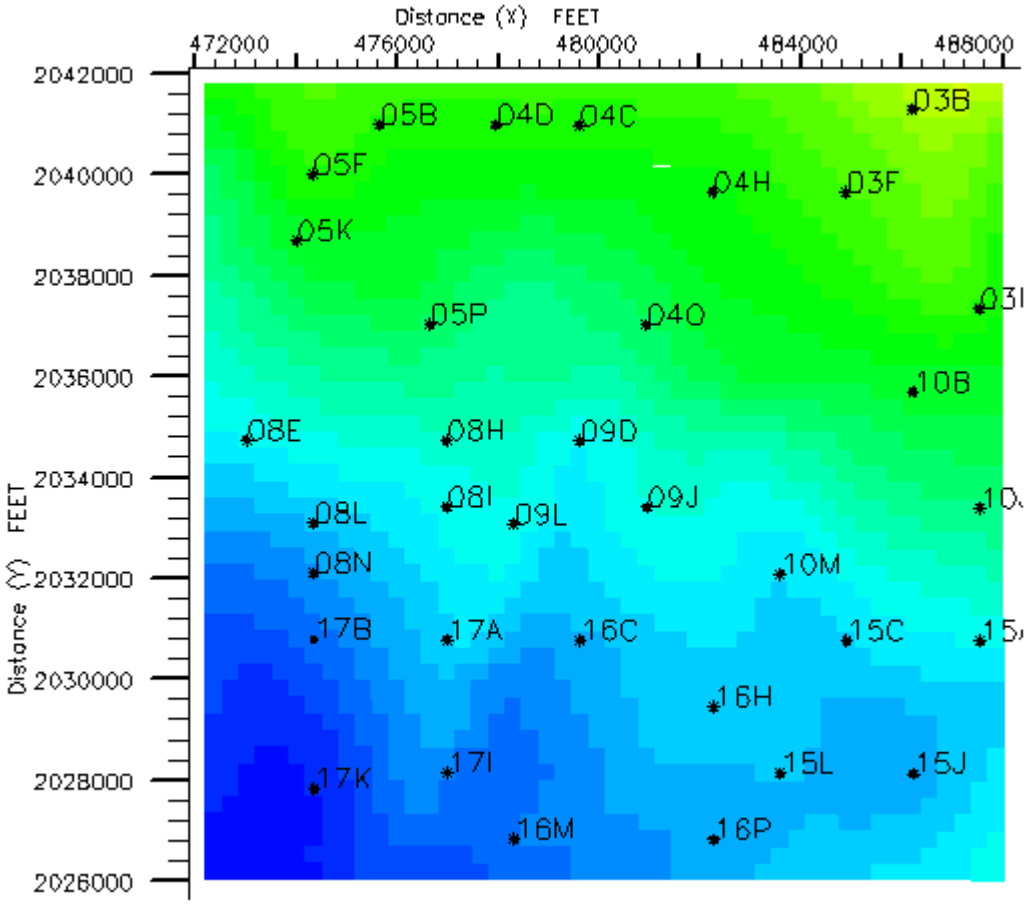


**Fig. 1** – Synthetic case well locations. This map shows the location of producing wells in the synthetic simulation model.

**Table 1** – Number of the Producing Wells as a Function of Time

| Date | Number of Producing Wells |
|---|---|
| January 1950 | 1 |
| January 1960 | 8 |
| January 1970 | 18 |
| January 1980 | 18 |
| January 1990 | 31 |
| January 2000 | 31 |
| January 2007 | 38 |

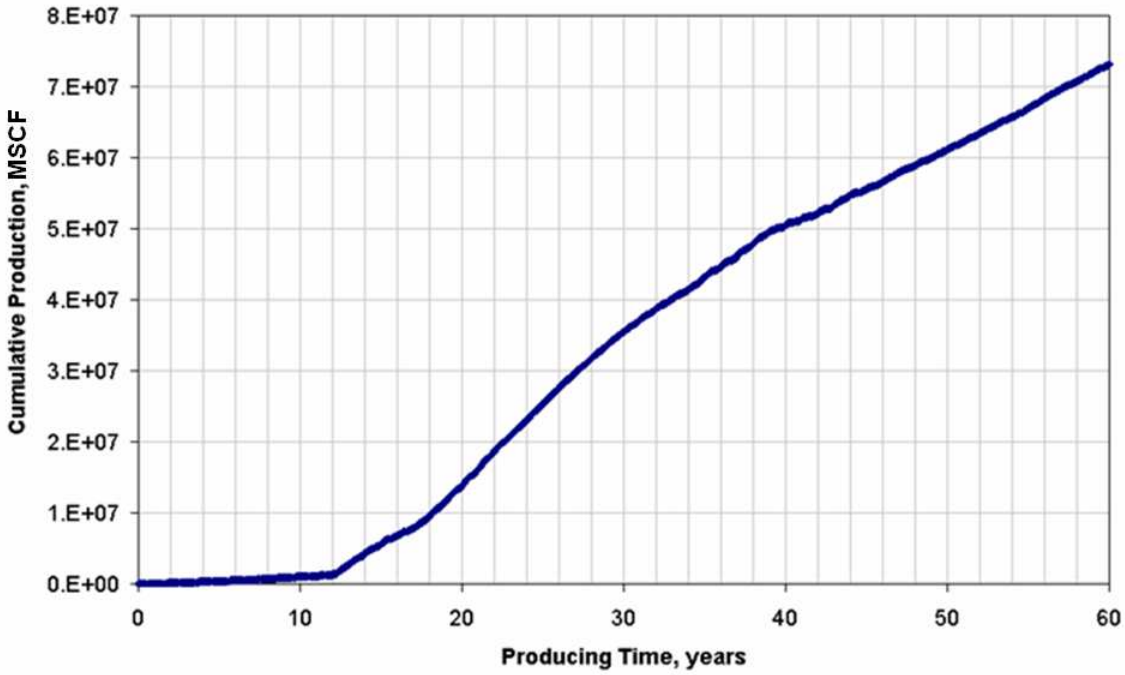


**Fig. 2** – Synthetic case historical gas production. Cumulative production is just around 73 Bscf.

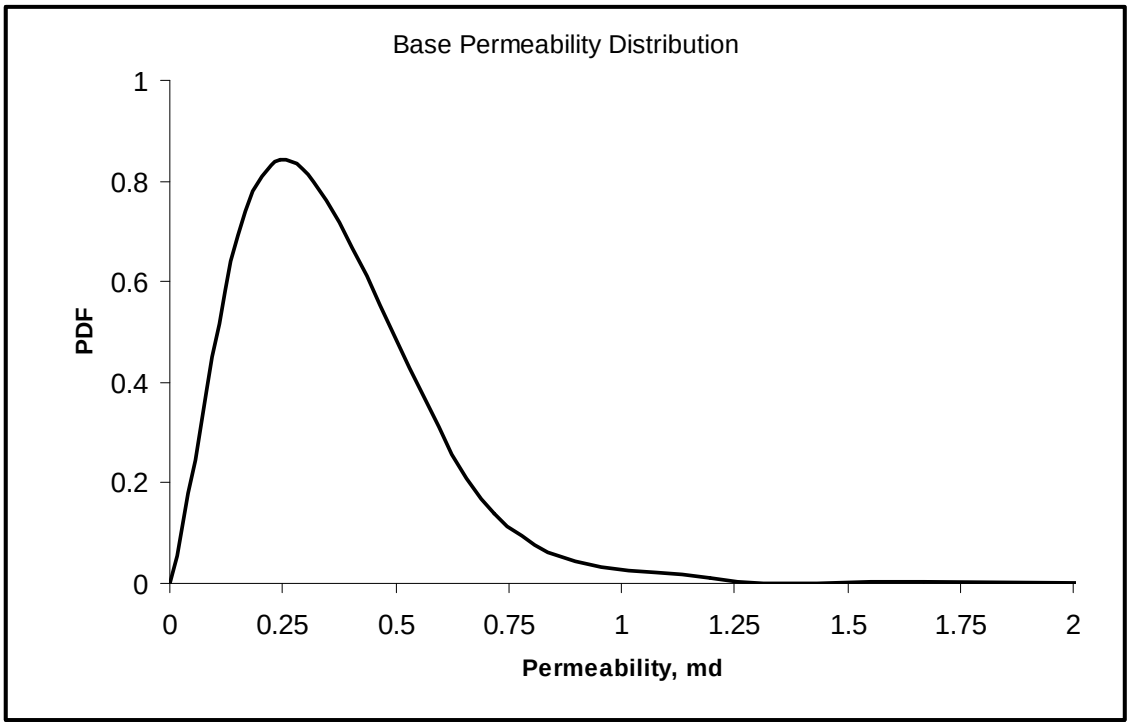


**Fig. 3** – Base permeability probability density function. This distribution was generated using the Gridstat geostatistical tool. This is a log-normal distribution with a mean of 0.3 and a standard deviation of 0.15.

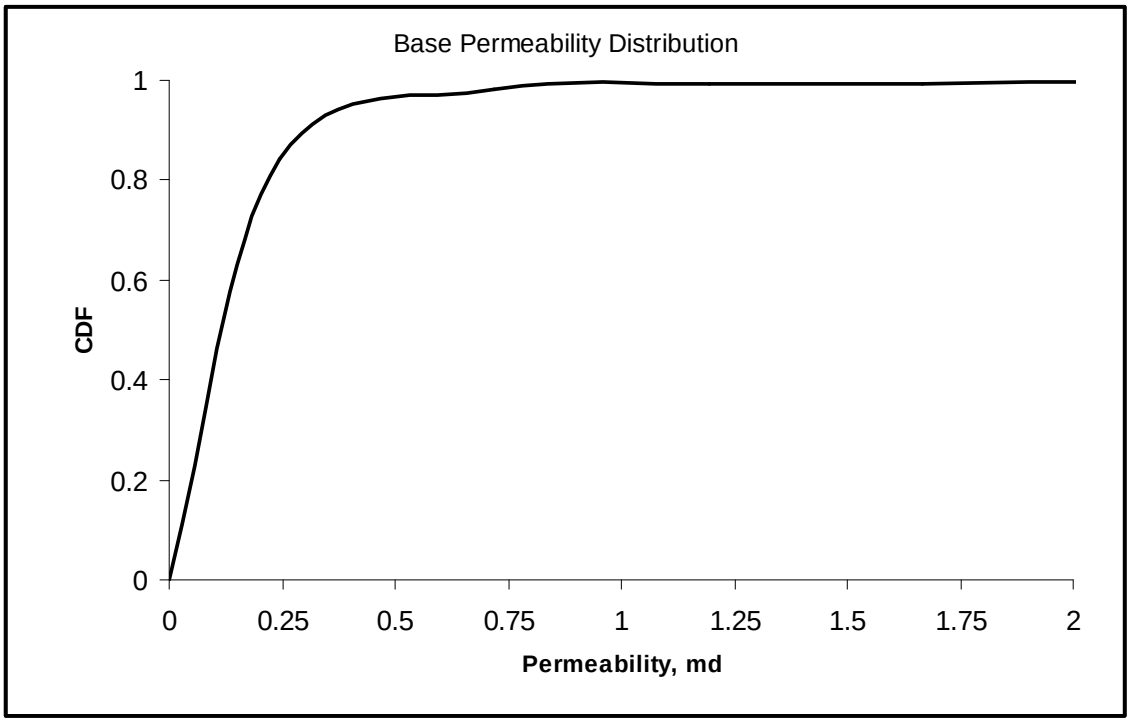


**Fig. 4** – Base permeability cumulative distribution function. This distribution was generated using the Gridstat geostatistical tool. This is a log-normal distribution with a mean of 0.3 and a standard deviation of 0.15.

**Table 2** – Power Law Coefficients and Derived Porosity Values.

| | **Minimum** | **Maximum** |
|---|---|---|
| Permeability | 0.008602 | 14.23 |
| Porosity | 0.04 | 0.12 |

| | **a** | **b** |
|---|---|---|
| Power Law Coefficients | 0.09356 | 0.025932 |

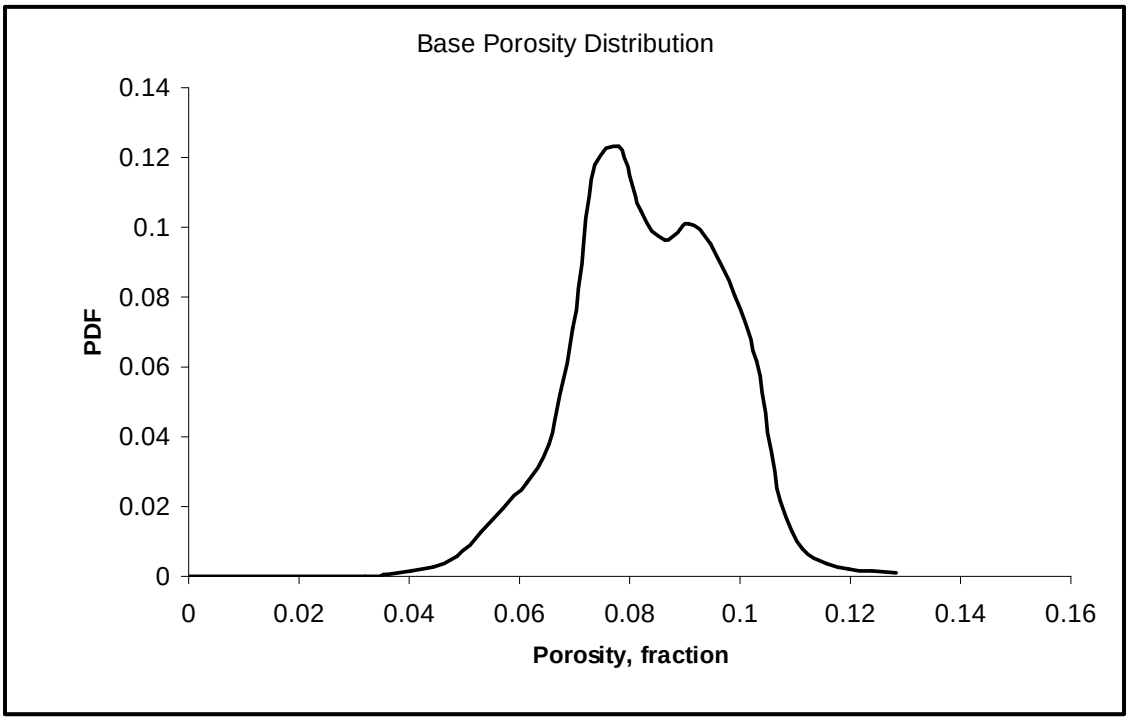


**Fig. 5** – Base porosity probability density function. This distribution was derived from the permeability distribution using a power law equation.

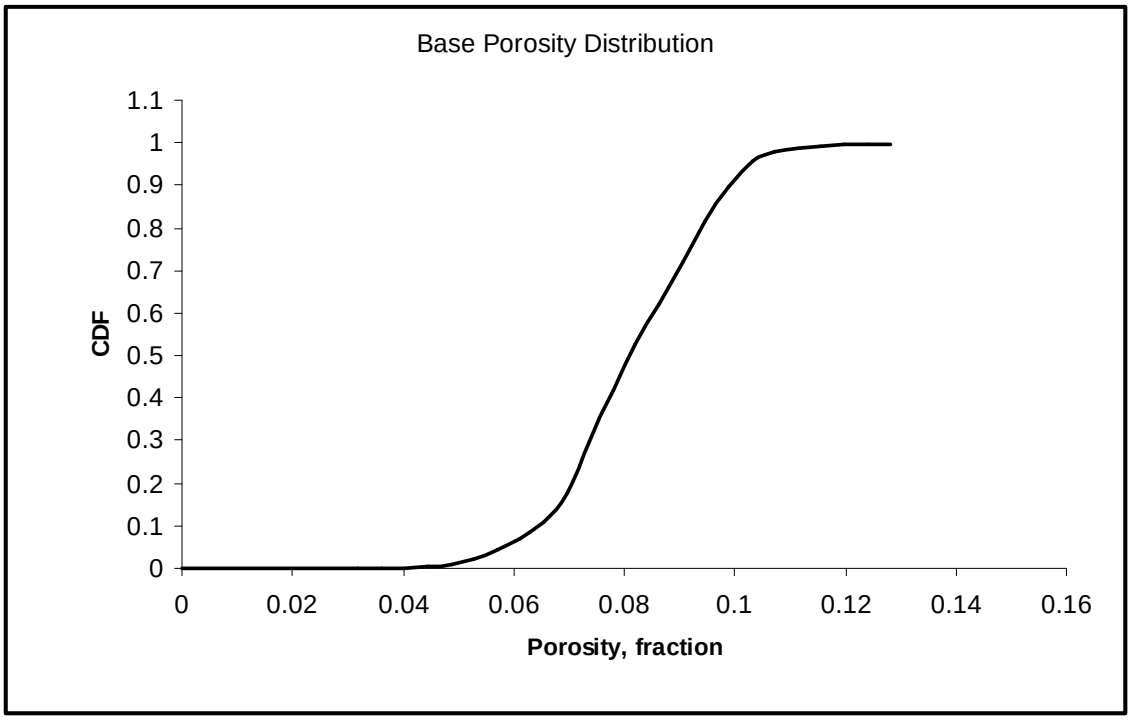


**Fig. 6** – Base porosity cumulative distribution function. This distribution was generated using a power law equation.

History Matching

In this section, I applied the sequential inversion method[13] to calibrate 150 initially prepared geostatistical reservoir models. These models have permeability distributions with a mean of 0.3 md and a standard deviation of 0.15 md. In the history matching process a correlation between porosity and permeability was not defined since there were no available core data. Hence, sequential inversion method modified only permeabilities. One example set of base permeability and porosity field maps and corresponding distributions can be seen in **Figs. 7-10**.

The initial pressure in this reservoir is estimated to be 2400 psi. A constant flowing bottomhole pressure of 300 psi is assumed. The same flowing bottomhole pressure was applied to each producing well.

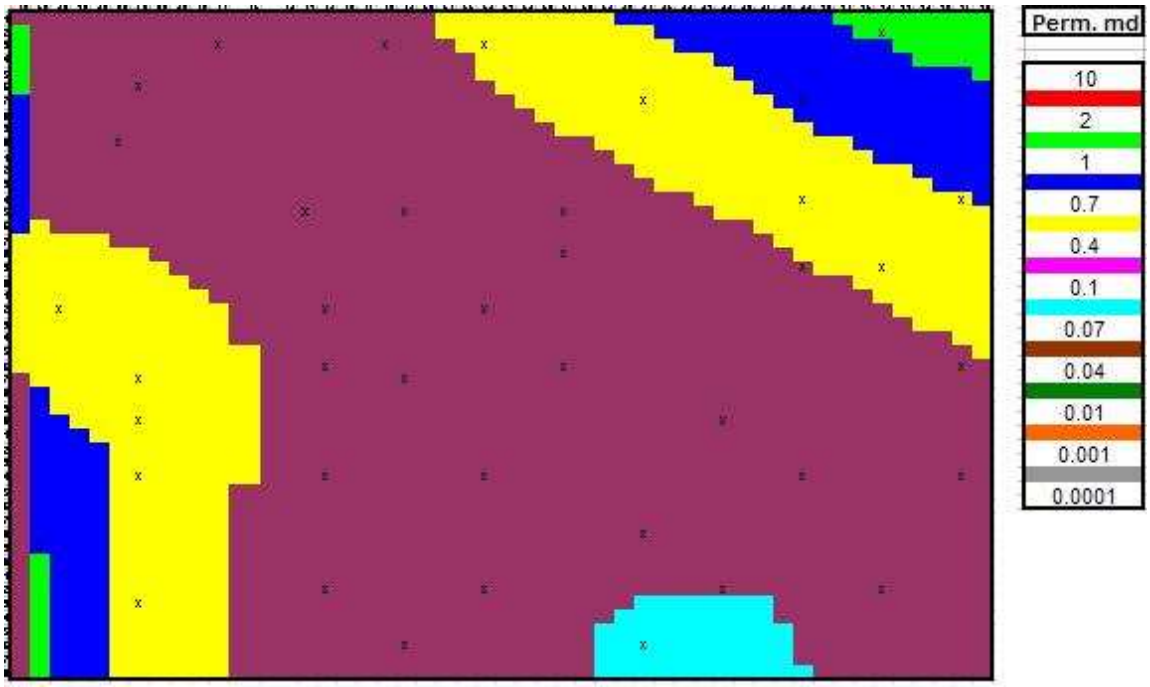


**Fig. 7** –A base permeability field map. Base permeability field of realization 25 generated with GridStat.

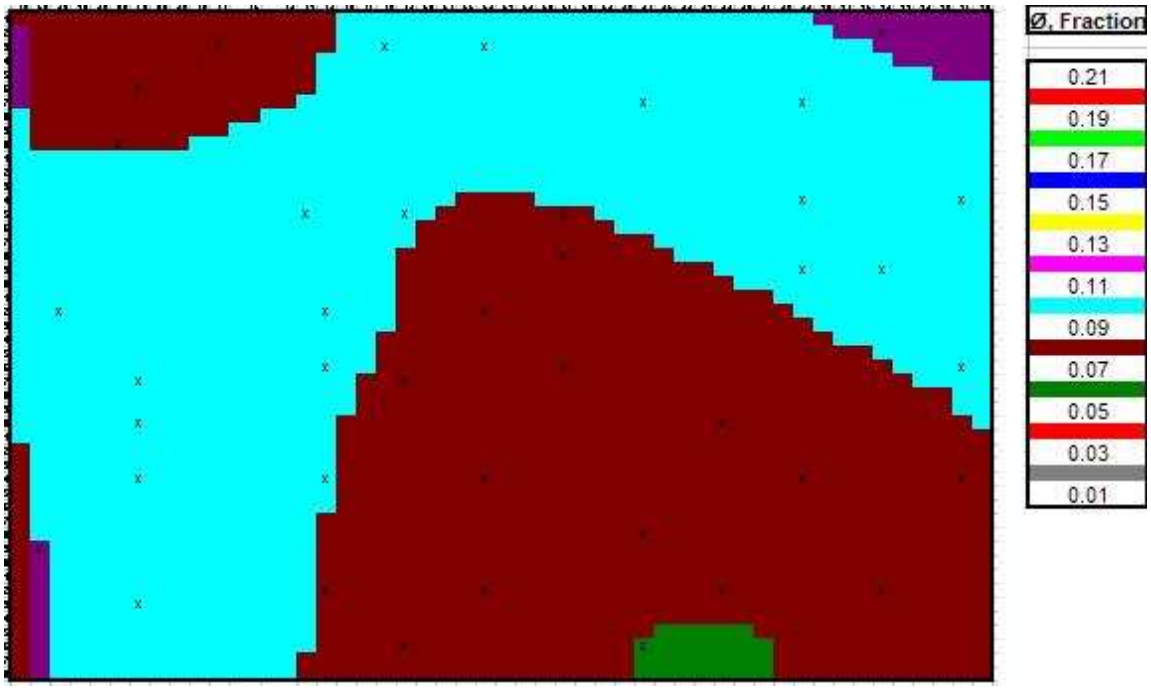


**Fig. 8** –A base porosity field map. Base porosity field of realization 25. This map was prepared using the corresponding permeability map and power law equation.

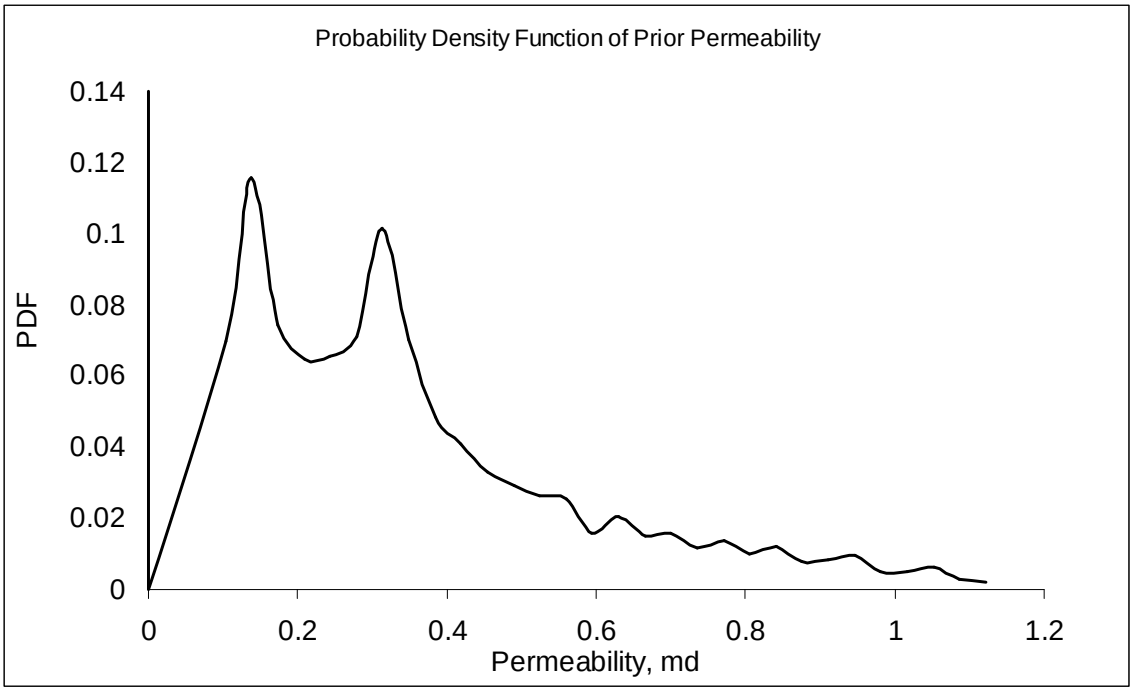


**Fig. 9** – Probability density function of the base permeability map. Probability density function of the base permeability values for the model shown in Fig. 7.

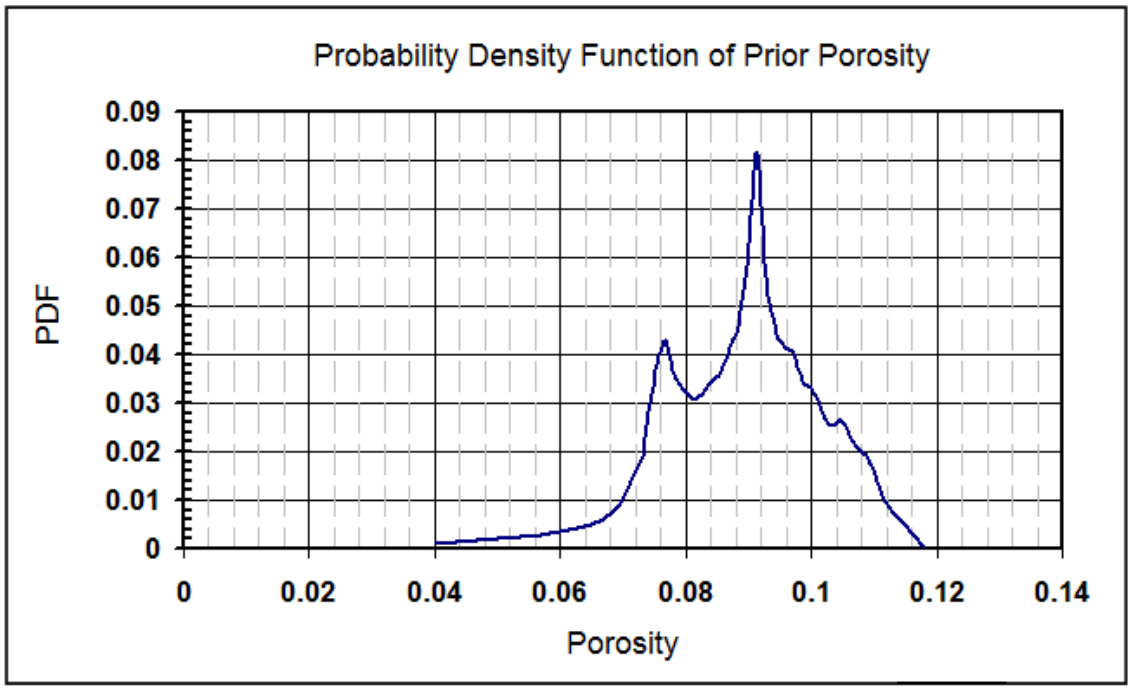


**Fig. 10** – Probability density function of the base porosity map. Probability density function of the base porosity values for the individual model shown in Fig. 8.

As mentioned above, 150 base models were used with sequential inversion method. Similar to other history matching methods, this method also includes objective function calculations. An objective function represents the amount of mismatch between simulated and observed data points. In general, objective function should decrease during the history matching process. Since I used actual production data of a multilayer reservoir in a single-layer model, I did not obtain steadily decreasing objective function profile. The general characteristic of the misfit function obtained in this work can be seen in **Fig. 11**. As can be seen here, misfit value can be lower at some points before the end of history matching. Therefore, it is crucial to select the models with the lowest misfit value. Thus, for each base model, an initial history matching was carried out to define the most optimum number of iterations. After defining the most optimum iteration numbers for each model, history matching processes were carried out to obtain best calibrated reservoir models. Difference in calculated and observed field production rates at the beginning and end of the history matching process can be seen in the figure on page 35.

After some test runs, it is observed that the lowest value of the objective functions were obtained at most at the end of 8 iterations. Hence, for the initial history match runs, 8 iterations were selected as the number of iterations. After evaluating the misfit function for each candidate, optimum numbers of iterations were obtained. In **Table 3** distribution of optimum iteration numbers can be seen. All 150 models were calibrated following this process. In **Figs. 12 - 13** we can see how sequential inversion method calibrated the realization-25 given in **Figs. 7** and **9**.

As mentioned earlier, in the history matching process, wells were constrained on flowing bottomhole pressure and matched on rate. However, in Eclipse runs, wells were primarily constrained on production rate, while a 100-psi bottomhole pressure constraint were used to prevent unrealistic rate and bottomhole pressure values during the simulation of the historical part. Hence, although we did not have perfect matches in the history matching phase, during the prediction runs we had the historical production data better represented because of the constraints used (**Figs. 14 – 15**).

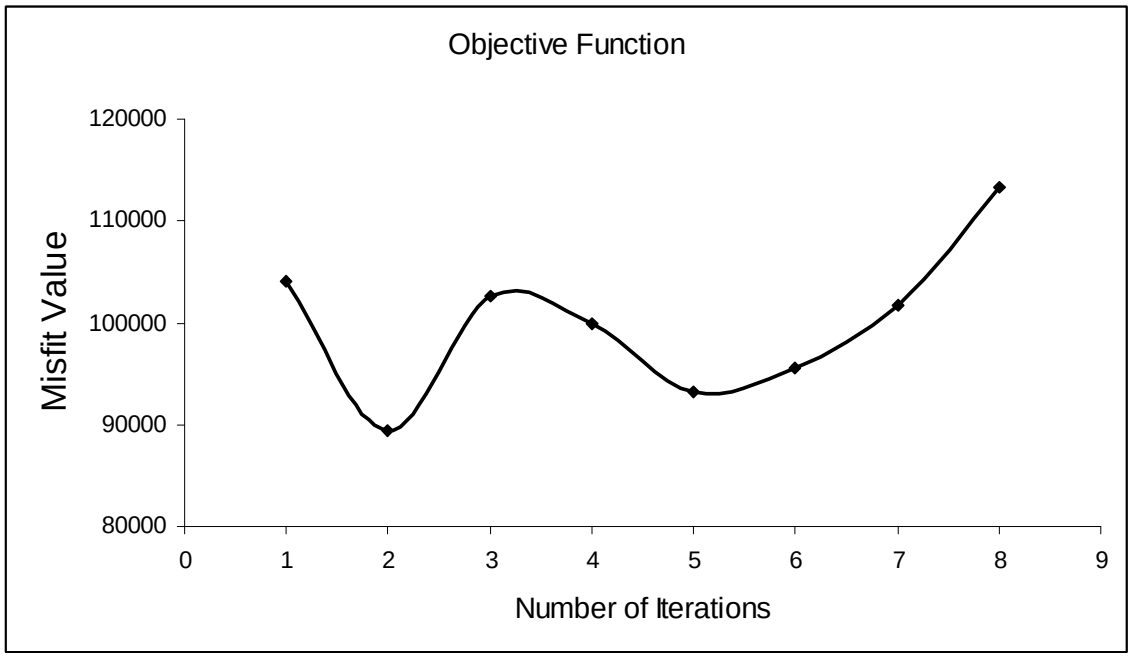


**Fig. 11** – Misfit function. Behavior of the misfit function during history matching process. In this example, second iteration was selected as the optimum number of iterations since it results with the lowest misfit value.

**Table 3** – Distribution of Optimum Iteration Numbers.

| Number of Iterations | Number of Models |
|---|---|
| 1 | 5 |
| 2 | 4 |
| 3 | 40 |
| 4 | 35 |
| 5 | 19 |
| 6 | 24 |
| 7 | 10 |
| 8 | 13 |

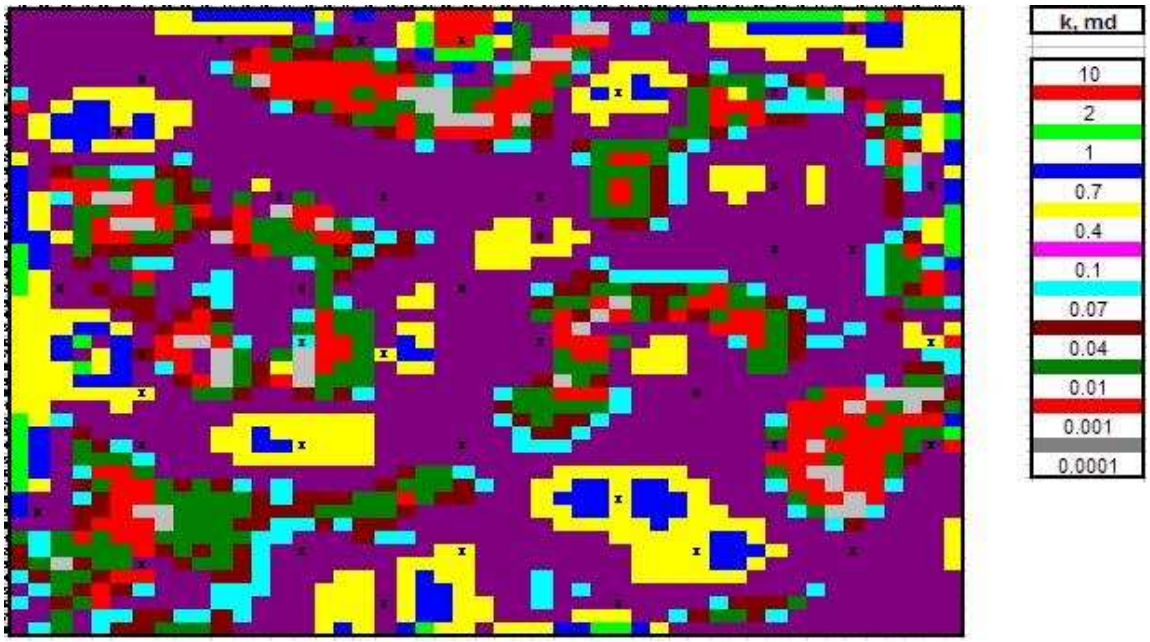


**Fig. 12** – Calibrated permeability field map. Calibrated permeability field of realization 25.

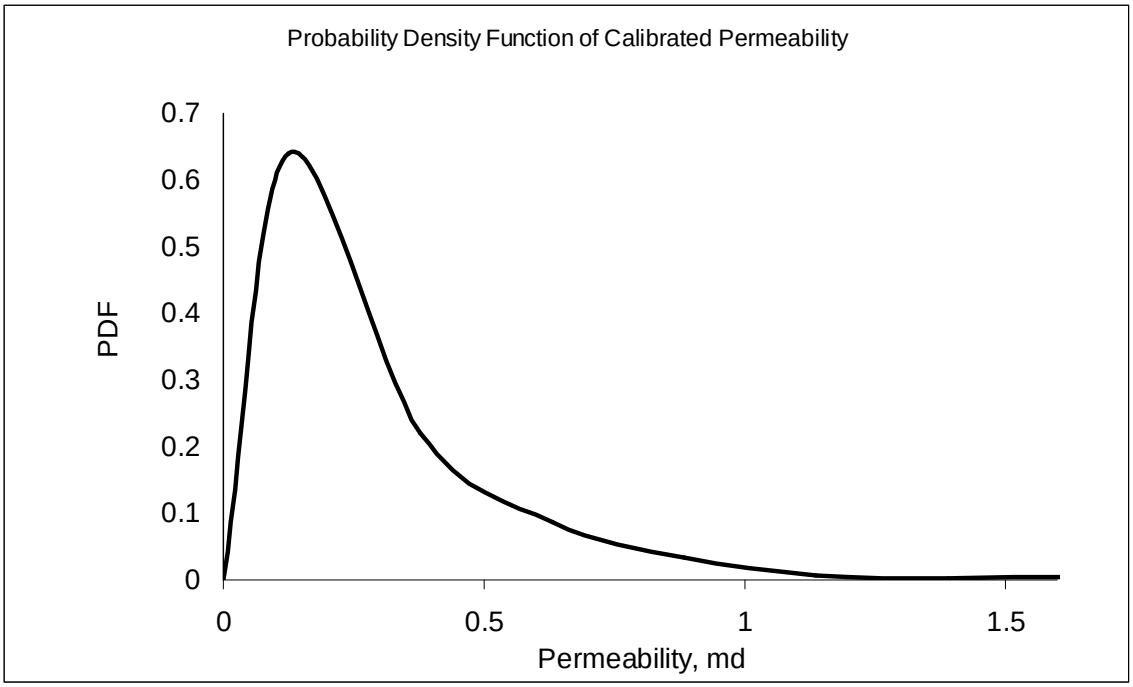


**Fig. 13** – Calibrated permeability probability density function. Calibrated probability density function of the base permeability values for the individual model 25.

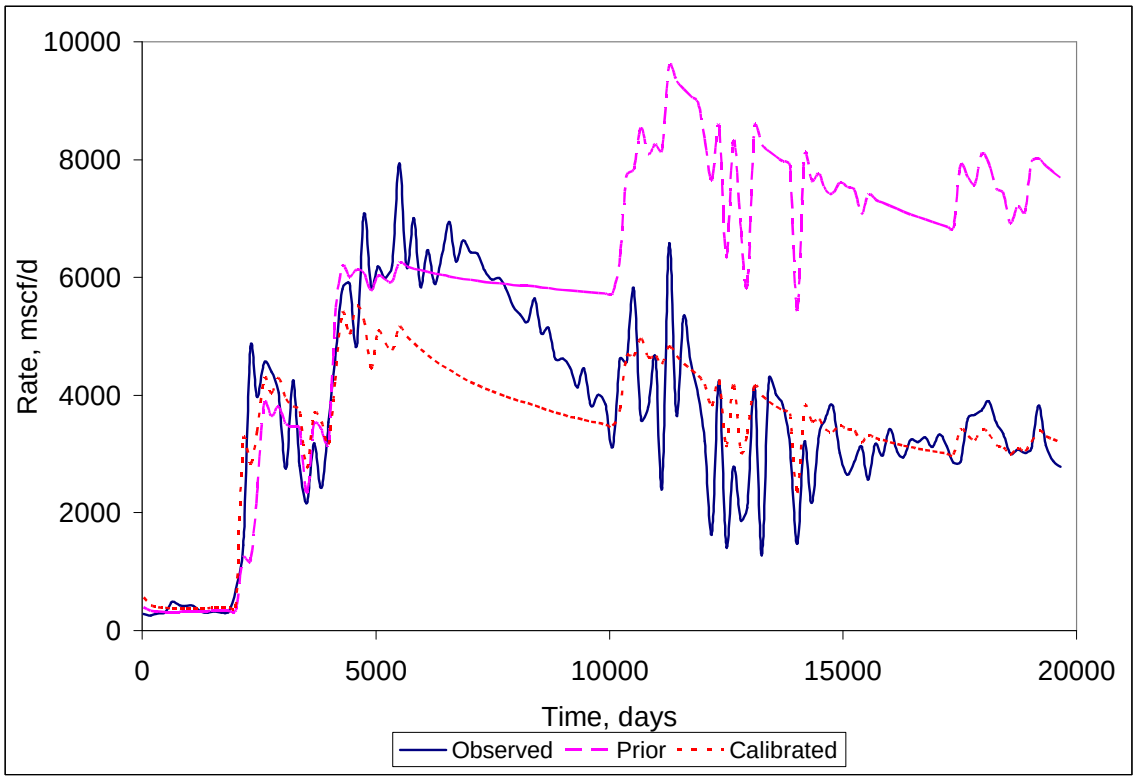


**Fig. 14** – Calculated and observed field production rates during history matching. Comparison of observed and calculated field cumulative production rates of Realization 25 in history matching process.

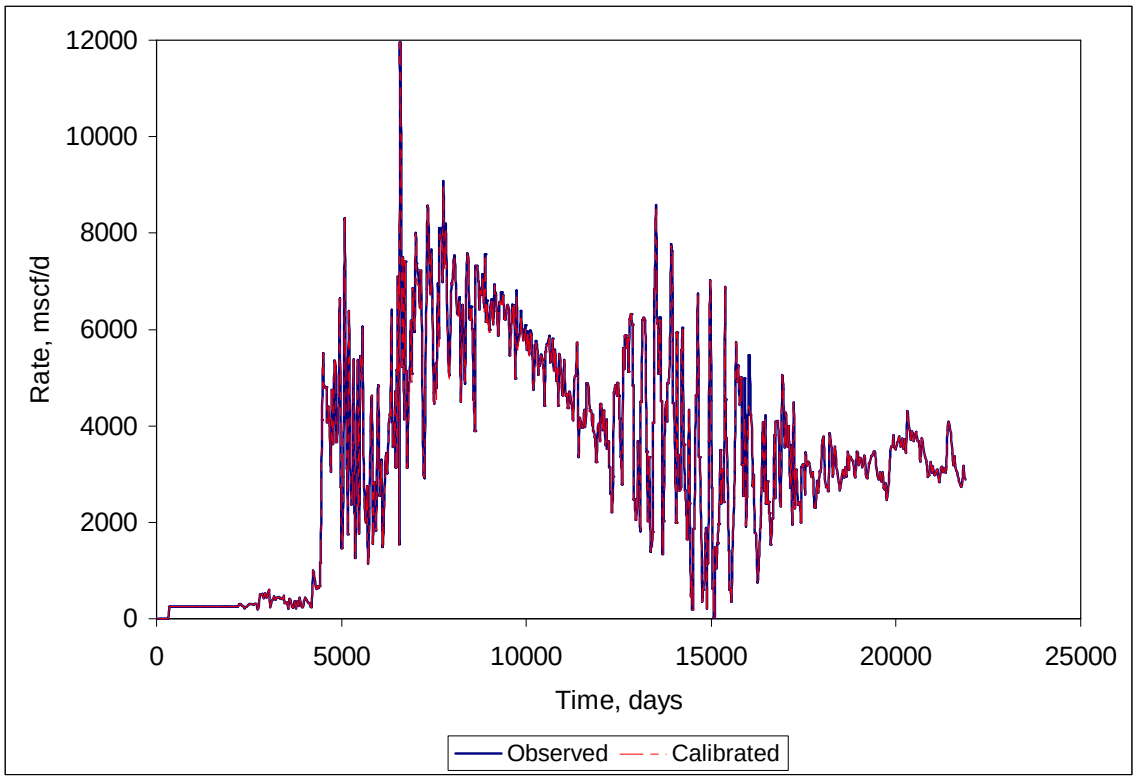


**Fig. 15** – Calculated and observed field production rates in Eclipse runs. Comparison of observed and calculated field cumulative production rates in Eclipse reservoir simulator. Early production data was not used in history matching process. In addition to that, to reduce the number of data points, one average production data used instead of four data point. Hence, compared to Fig. 14, this plot is noisier and it has longer production profile.

Performance Prediction

In sequential inversion approach, wells are constrained on the pressure and matched on the production rate. However, since only production data was available, I had to assume a constant flowing bottomhole pressure value for the history matching process. In Eclipse simulations, before predicting the reservoir performance we need to simulate the historical part. While simulating the historical performance in Eclipse, I used production data as a primary constraint.

Cumulative production from the reservoir in its 60 years of life is around 74 Bscf. While simulating historical data in Eclipse, I observed that the simulator could not match the cumulative historical production with the models that gave high misfit values during the history matching. Hence, calibrated realizations with a misfit value higher than 90,000 and a cumulative historical production lower than 73 Bscf in Eclipse runs were excluded. The purpose of the filtering is to prevent the forecast from being unrealistic. **Fig. 16** shows the distribution of misfit values from history matching with their corresponding cumulative production values obtained from Eclipse runs. After applying the misfit and cumulative production constraints, 74 calibrated models remained for probabilistic infill well location determination.

Remaining models were used to predict reservoir's future performance with Eclipse simulator. A base case performance prediction run is made with the existing wells to evaluate the performance of the reservoir without any infill well. At the end of historical part, I changed the production rate constraint into to pressure. If I kept using rate constraint in prediction part, wells would continue to produce with last production-

rate data. The same constant bottomhole pressure profile was used for each well in the reservoir **Table 4**. At the beginning of prediction, a pressure and saturation map were saved to reduce the simulation time for the subsequent predictions. Next, the schedule file was updated and an infill well was placed in the first grid block. A prediction run was made with one infill well besides existing wells. This process was repeated on every grid block which does not have an existing well. Since, the model has 2304 cells and 40 production wells, 2265 prediction runs were made for each realization. Although the number of simulations was so large, I constructed and used an operating code to modify schedule and grid property files and capture results in files which reduced the simulation time considerably. On a typical desktop computer, 2265 forecast runs took around 3 hours. Use of multiple computers reduced the total simulation and processing time to less than a week.

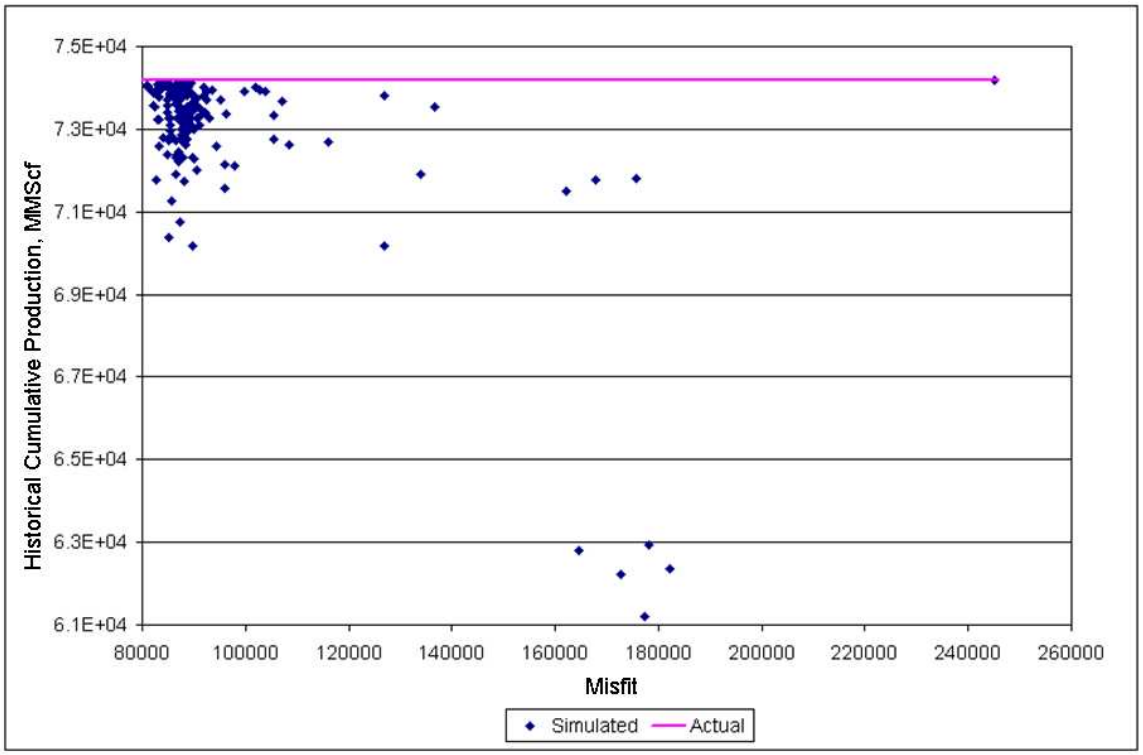


**Fig. 16** – Distribution of the misfit function values. Simulated historical cumulative production versus corresponding misfit value. Calibrated reservoir models were run in Eclipse black oil simulator and historical cumulative productions were observed.

**Table 4** – Pressure and Rate Constraints in Performance Predictions.

| Date, Years | BHP, psi |
|---|---|
| 0 | 650 |
| 4 | 600 |
| 8 | 550 |
| 12 | 500 |
| 16 | 450 |

## Discounted Incremental Field Production Calculation

Forecasted field cumulative production values for each run were stored at discrete points in time specifically the $2^{nd}$, $5^{th}$, $10^{th}$, $15^{th}$ and $20^{th}$ years. These values were used to calculate discounted incremental field production, as described earlier.

This process gave us the discounted incremental field production due to infill well in each possible location, considering the interference effects between the infill well and existing wells for a given realization. In this work, I conducted this methodology on 74 calibrated reservoir models. Hence, discounted incremental field production was calculated 74 times for each grid block, which allowed me to generate a distribution of forecasted incremental field for each grid block.

## Evaluation of the Results

Every grid block that does not contain an existing well is a candidate location for an infill well. As mentioned in the previous section, distributions of discounted incremental field production were generated for all candidate locations. Descriptive statistical analysis was used to evaluate the distributions. In this study, I focused on mean and standard deviation values to compare the performance of infill wells. For every candidate location, a mean and standard deviation of the discounted incremental field production distribution was calculated. A map of the mean of discounted incremental field production is shown in **Fig. 17**. In this map, two regions containing the highest mean values have been circled. These regions indicate the possible location of an infill candidate that might bring the largest incremental production. However, the quality

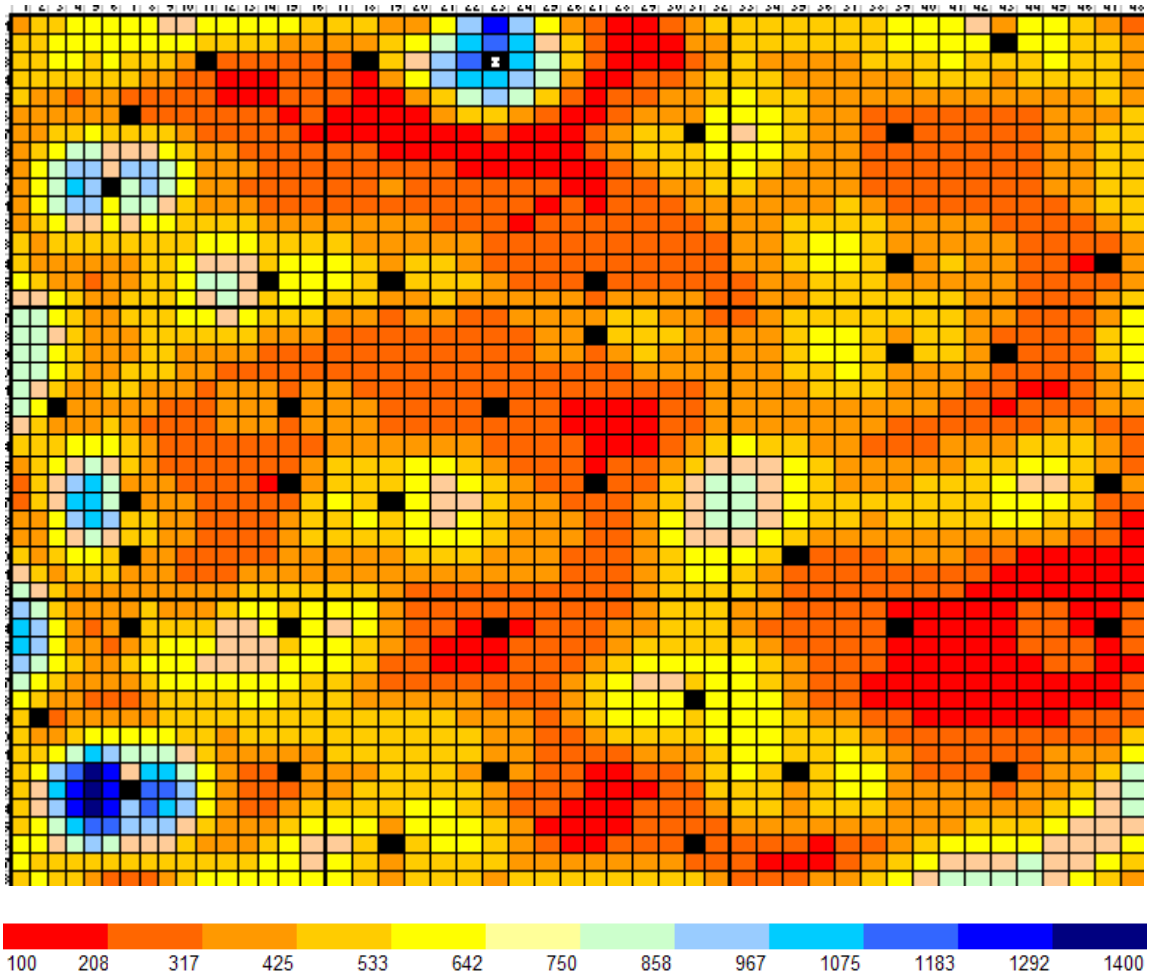


**Fig. 17** – A map representing the mean values of the IFP. Map of the mean of discounted incremental field production (MMscf). In this figure black cells represent the cells with existing wells. The cell with white 'X' contains an exiting well that is not currently producing.

of a decision based on only the mean values may be poor depending on the risk preference of the operator. Hence, it is wise to consider the associated uncertainty before making a decision. In **Fig. 18** a map of the standard deviations in discounted incremental production can be seen. **Figs. 17** and **18** show that, the regions with greater mean values also have greater standard deviation values. In other words, the regions promising more additional reserves have greater associated risk. The performance index map was generated by calculating the ratio of mean to standard deviation for each cell (**Fig. 19)**. The performance index represents the amount of discounted incremental production per unit risk. Although all those maps are helpful in the evaluation of the results, if they are considered in decision-making process individually the final decision may be poor.

In addition to those maps, I have cross-plotted the mean and standard deviation values (**Fig. 20)**. This plot more information about the distributions of discounted incremental field production. Each data point in **Fig.20** represents a grid block which does not have an existing well. In this work, I assumed an arbitrary economic limit as an infill selection criterion. I chose 680 MMscf discounted incremental production as the economic limit and considered the lower values to be unfeasible infill candidates and, colored them in blue. I colored the data points above the economic limit in red and green. A green color code was used to represent those grid blocks on the efficient frontier, i.e., grid blocks with minimum standard deviation (uncertainty) for a given mean. If we were to choose infill locations with minimum risk, we would focus on grid blocks located on the efficient frontier in the mean-standard deviation cross-plot.

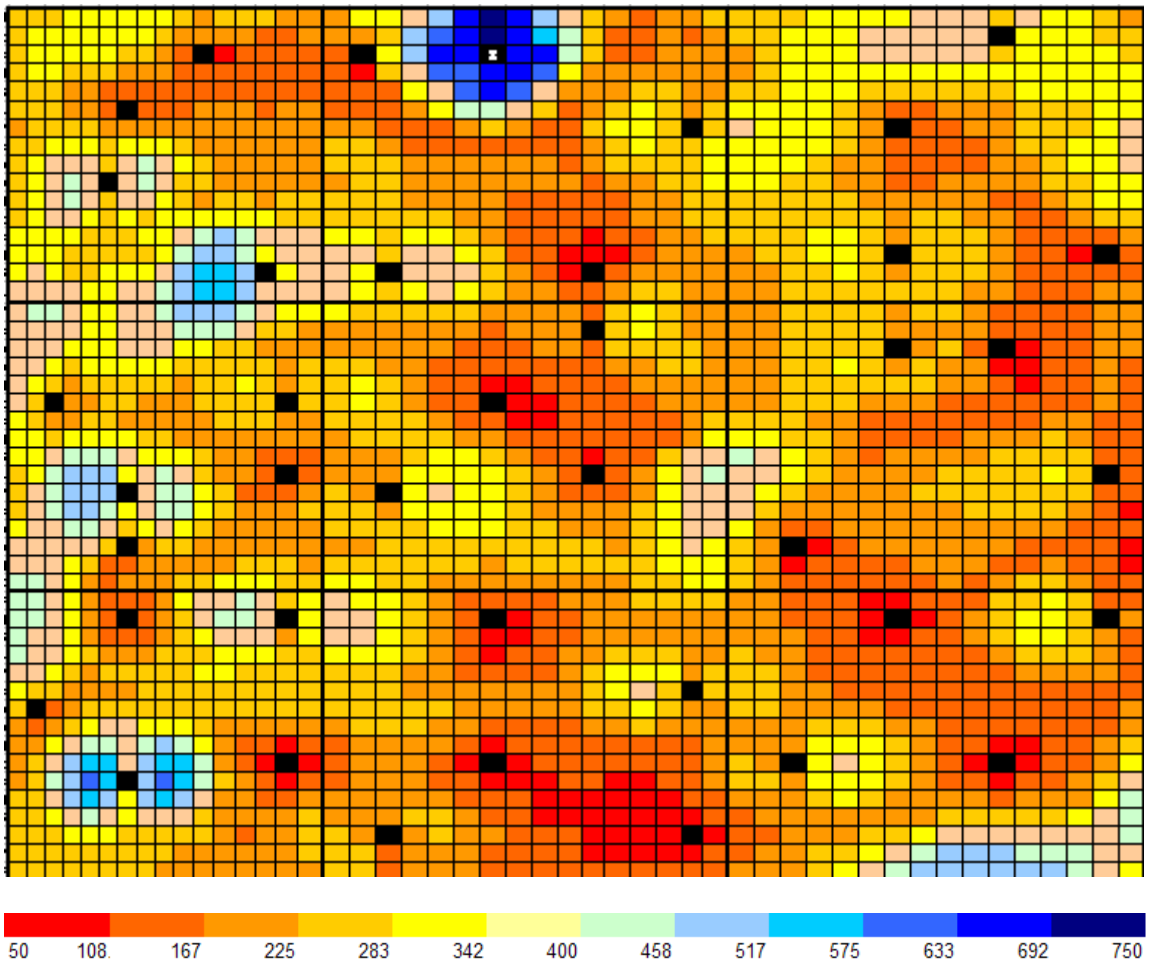


**Fig. 18** – A map representing the standard deviation values of the IFP. Map of the standard deviation of discounted incremental field production (MMscf). In this figure black cells represents the cells with existing wells.

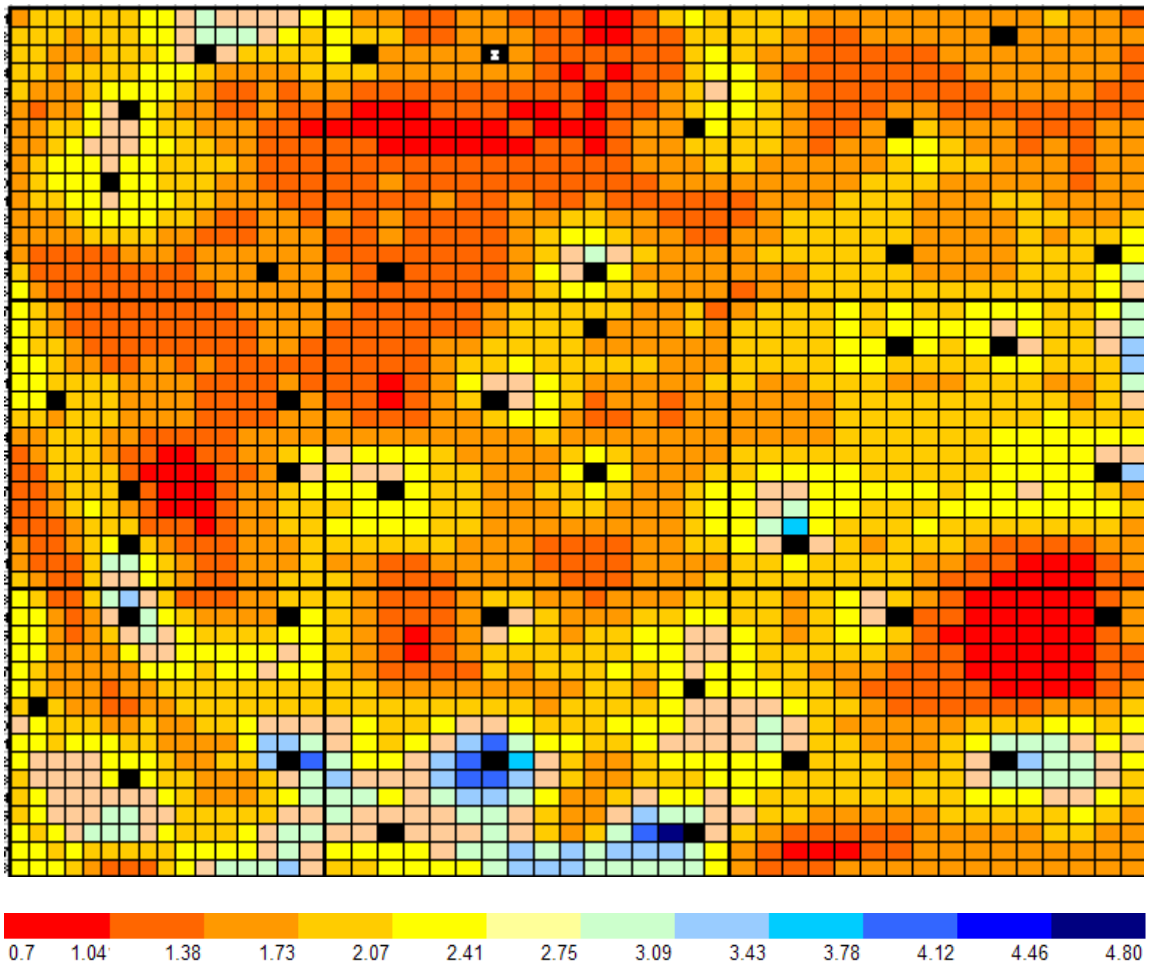


**Fig. 19** – Performance index map. Performance index is the ratio of the mean of the discounted incremental production to the standard deviation.

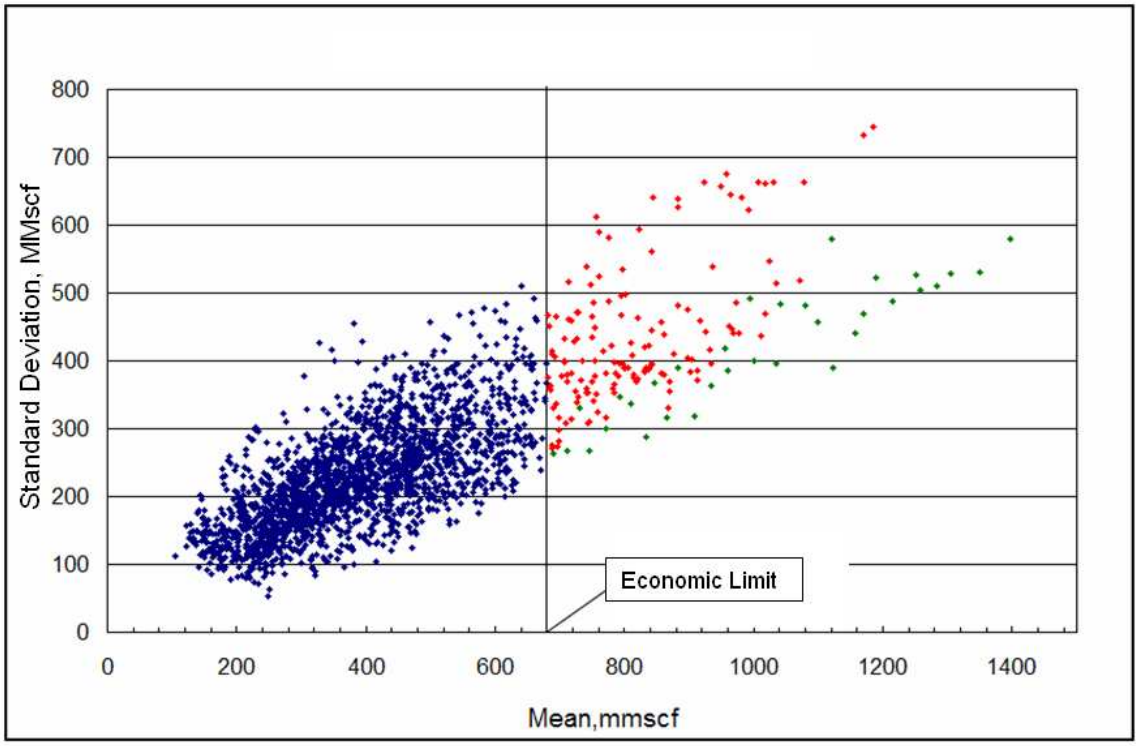


**Fig. 20** – Cross-plot of the mean and standard deviation of the IFP.

However, since some operators may be risk-seeking, I considered all grid blocks with a discounted incremental cumulative production greater than the economic limit to be an infill candidate. In **Fig. 21** candidate locations can be seen on the simulation grid in red and green colors. As in Fig. 21, a green color represents the grid blocks on the efficient frontier and a red color represents a grid block that brings incremental production more than the economic limit.

As can be seen in **Fig. 21**, most of the viable infill candidate locations are near existing wells, which is counter to my expectations. I would expect, the viable locations would be far away from the existing wells. I believe the reason for this result is a underestimation of uncertainty in the prior permeability distribution. To explain the effect of the prior permeability distribution, I plotted the distributions of permeabilities in the nine-cell blocks around all existing wells. Since we have 40 existing wells, distributions of permeability were generated with 360 permeability values.

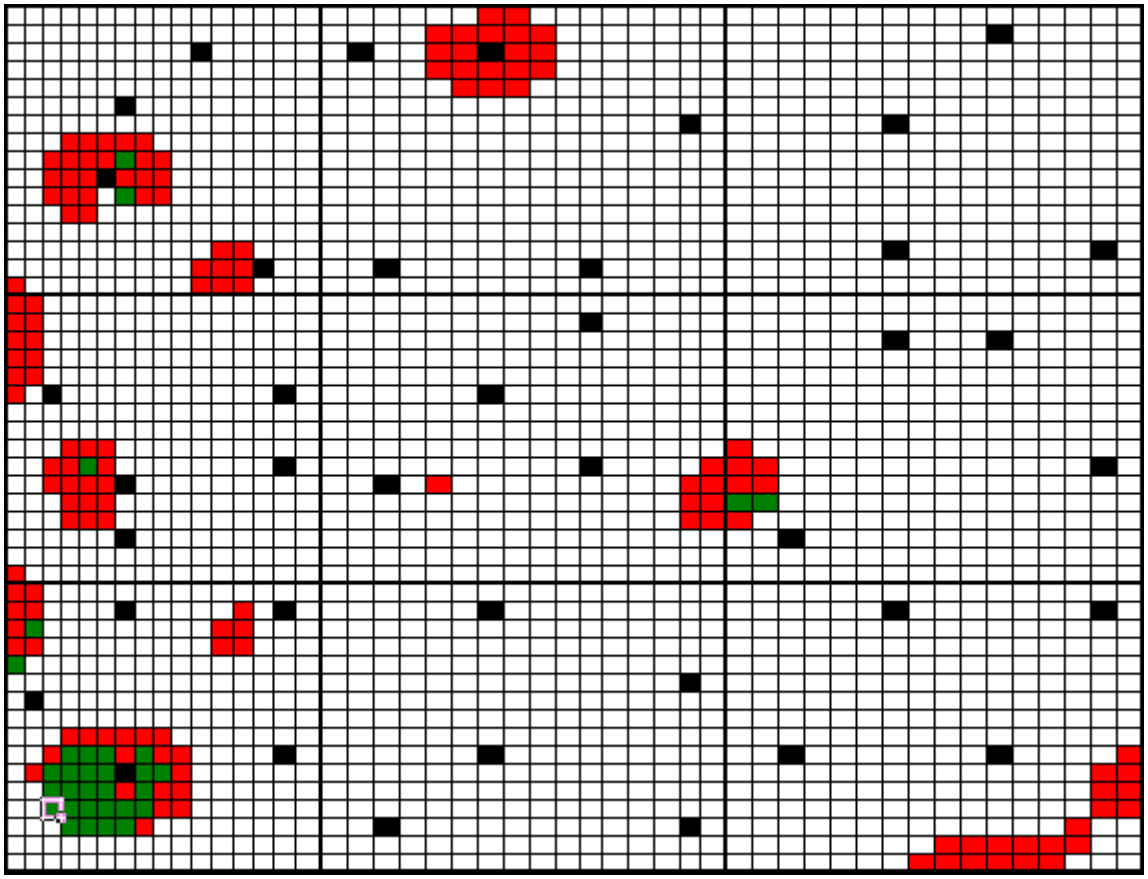

**Fig. 21** – Infill candidate locations on simulation grid. Red and green grids represent the possible locations for the infill candidates which have larger incremental production than the economic limit. Green grids represent the data points on the efficient frontier in Fig. 20.

Prior and posterior (before and after history matching) distributions were compared for two different realizations. As can be seen in **Fig. 22**, permeability near existing wells increases significantly after history matching, in many cases beyond the range of uncertainty in the prior permeability distribution. This indicates that the uncertainty in permeability in prior models was underestimated. While permeability values around existing wells were increasing, permeability values in cells far from wells did not change or changed only a little bit **(Fig. 23)**. Therefore, as a result of underestimating the uncertainty in prior permeability models, I obtained regions with higher permeability around existing wells. In turn, although it is not likely, the best locations for the infill candidates were found around existing wells.

Underestimation of uncertainty in prior permeability distribution resulted in invalid results. I should have considered a larger uncertainty range for the prior permeability distribution to ignore this problem.

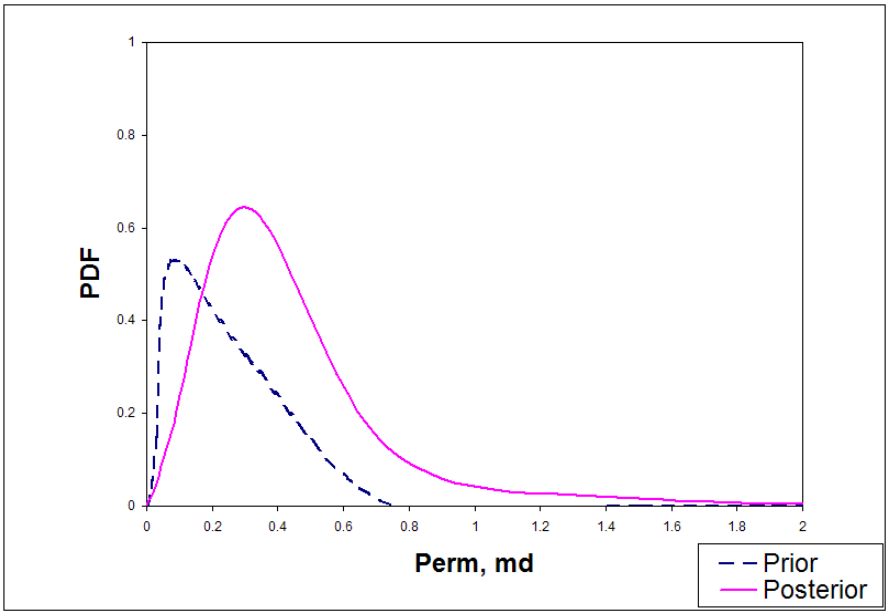


Model 70

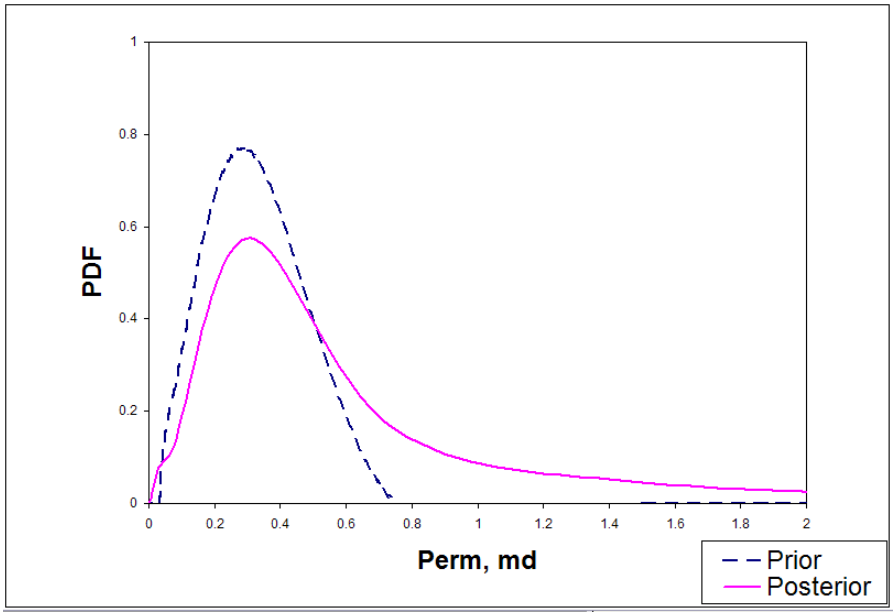


Model 82

**Fig. 22** – Comparison of the permeability distributions around the wells. Comparison of the prior and posterior permeability distributions of the surrounding grids around the existing wells, for two different realizations.

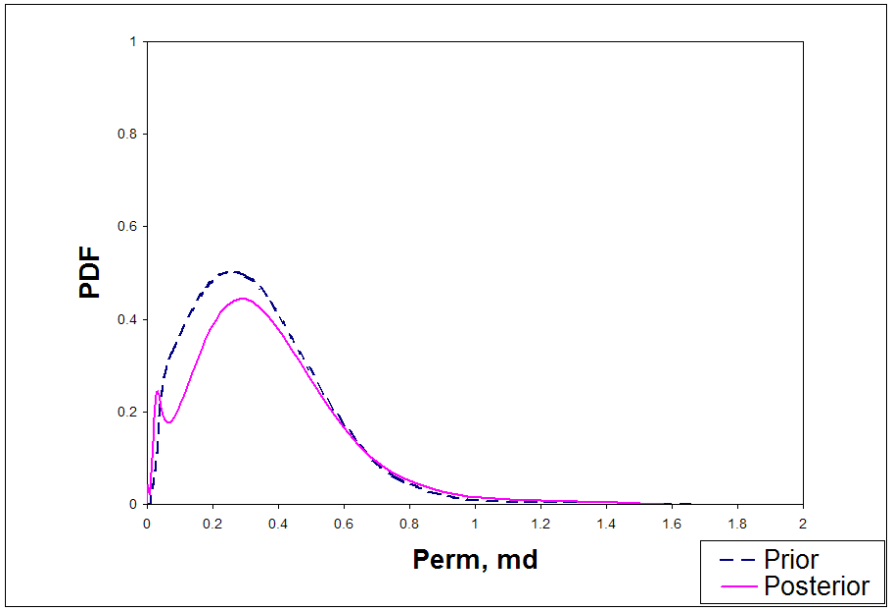


Model 70

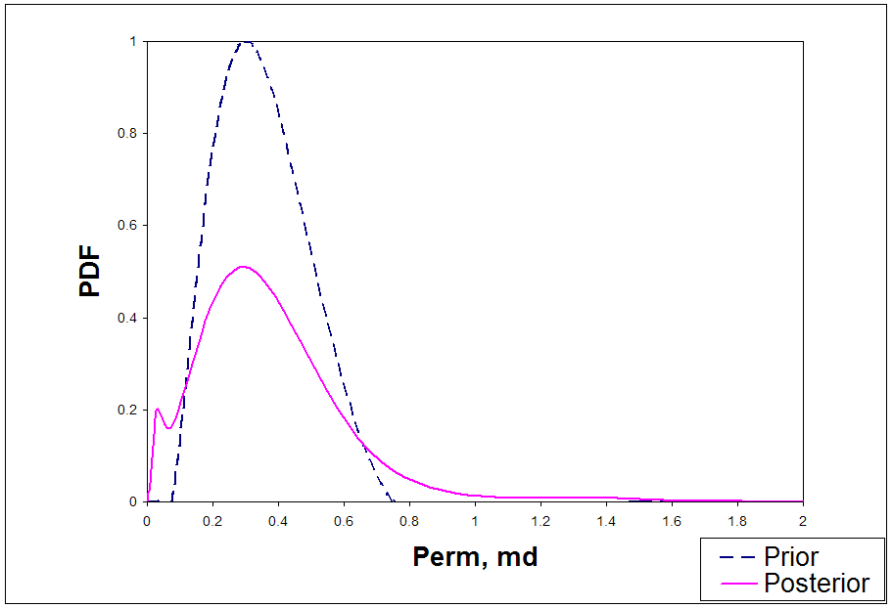


Model 82

**Fig. 23** – Comparison of the permeability distributions of all reservoirs. Comparison of the prior and posterior permeability distributions for two different realizations.

## Summary of Results

This synthetic test demonstrates uncertainty quantification in infill location selection. By using many realizations, we are able to quantify the uncertainty in the reservoir description. This gives us an opportunity to quantify uncertainties in the forecasts. In this work, underestimation of uncertainty in our prior models resulted in unreasonable infill locations.

# CONCLUSIONS AND RECOMMENDATIONS

## Conclusions

Uncertainty quantification in infill location selection is a promising approach for reservoir management. We can draw the following conclusions from the test described above:

1. The synthetic study demonstrates that we can quantify uncertainty in our forecasts by using multiple realizations.

2. Use of live production data in test study demonstrates that the probabilistic approach is feasible and practical for use on actual fields and could be applied to real world problems.

3. This study demonstrates that underestimation of uncertainty in our prior reservoir simulation models can cause invalid results in probabilistic infill location determination problem.

## Recommendations for Future Work

The results of this research did not work out very well. In order to improve the results, the problems addressed in the thesis body should be investigated.

To the best of my knowledge, the new researcher who is going to develop this work should make sure that the uncertainty in the prior models is not underestimated. One way to do it would be to compare the prior and posterior (before and after history matching) distributions of the permeability, around the wells and of the whole reservoir prior to performance prediction. In those distributions, prior models should be able cover at least the same uncertainty ranges with the posterior models.

# NOMENCLATURE

$k_i$ = Permeability of the $i^{th}$ grid block

$A$ = Matrix of flow elements

$p$ = Vector of well block pressures

$b$ = Known pressures

$q$ = Flow rate

$J$ = Productivity index

$p_{wf}$ = Flowing bottomhole pressure

$IFP$ = Incremental field production

BHP = Bottomhole pressure

GPST = Generalized pulse-spectrum technique

# REFERENCES

1. Wiggins, R.L. and Startzman, R.A.: “An Approach to Reservoir Management,” paper SPE 20747 presented at the 1990 SPE Annual Technical Conference and Exhibition, New Orleans, 23-26 September.

2. Holmes, J.C., McVay, D.A., and Senel, O.: “A System for Continuous Reservoir Simulation Model Updating and Forecasting,” paper SPE 107566 presented at the 2007 SPE Digital Energy Conference and Exhibition, Houston, Texas, 11-12 April.

3. Capen, E.C.: “The Difficulty of Quantifying Uncertainty,” *JPT* (August 1976) 843.

4. Floris, F.J.T.,Bush, M.D., Cuypers, M., Roggero, F., and Syversveen, A.R.: “Methods for Quantifying the Uncertainty of Production Forecasts: A Comparative Study,” *Petroleum Geoscience* (2001) **7**, S87.

5. Beckner, B.L. and Song, X.: “Field Development Planning Using Simulated Annealing-Optimal Economic Well Scheduling and Placement,” paper SPE 30650 presented at 1995 the SPE Annual Technical Conference and Exhibition, Dallas, 22-25 October.

6. Farnstrom, K. L. and Litvak, M. L.: “Automatic Simulation Algorithm for Appraisal of Future Infill Development Potential of Prudhoe Bay,” paper SPE 59374 presented at 2000 the SPE/DOE Improved Oil Recovery Symposium, Tulsa, 3-5 April.

7. McCain, W.D. Jr., Voneiff, G.W., Hunt, E. and Semmelbeck, M.E.: “A Tight Gas Field Study: Carthage Field,” paper presented at the 1993 SPE 26141 Gas Technology Symposium, Calgary, 28-30 June.

8. Voneiff, G.W. and Cipolla, C.: “A New Approach to Large-Scale Infill Evaluations Applied to the Ozana Gas Field,” paper SPE 35203 presented at the 1996 SPE Permian Oil and Gas Recovery Conference, Midland, Texas, 27-29 March.

9. Guan, L., McVay, D.A., Jensen, J.L., and Voneiff, G.W.: ”Evaluation of a Statistical Infill Candidate Selection Technique,” paper SPE 75718 presented at the 2002 SPE Gas Technology Symposium, Calgary, Alberta, April 30-May 2.

10. Badru, O. and Kabir, C.S.: ”Well Placement Optimization in Field Development,” paper SPE 84191 presented at the 2003 SPE Annual Technical Conference and Exhibition, Denver, 5-8 October.

11. Gao, H. and McVay, D.A.: “Gas Infill Well Selection Using Rapid Inversion Methods,” paper SPE 90545 presented at the 1996 SPE Annual Technical Conference and Exhibition, Houston, Texas, 26-29 September.

12. Cheng, Y., McVay, D.A., Wang, J., and Ayers, W.B.: “Simulation-Base Technology for Rapid Assessment of Redevolepment Potential in Stripper-Gas-Well Field – Technology Advances and Validation in the Garden Plains Field, Western Canada Sedimentary Basin,” paper SPE 100583 presented at the 2006 SPE Gas Technology Symposium, Calgary, Alberta, 15-17 May.

13. Guyaguler, B. and Horne, R.N.: “Uncertainty Assessment of Well-Placement Optimization,” paper SPE 87663 presented at the 2001 SPE Annual Technical Conference and Exhibition, New Orleans, 30 September-3 October.

14. Cheng, Y., McVay, D.A., and Lee, W.J.: “Optimal Infill Drilling Design for Marginal Gas Reservoirs Using a Simulation-Base Inversion Approach,” paper SPE 104574 presented at the 2006 SPE Eastern Regional Meeting, Canton, Ohio, 11-13 October.

15. Allard, D.N., Hilyer, M.G., Gerbacia, W.E., and Rychener, L.M.: “Empirical Risk Assessment of Infil Drilling Locations, Barow Island, Australia,” paper SPE 56816 presented at the 1999 SPE Annual Technical Conference and Exhibition, Houston, 3-6 October.

16. Guyaguler, B., Horne, R.N., Rogers, L., Livermore, L., and Rosonzweig, J.J.: “Optimization of Well Performance in a Gulf of Mexico Waterflooding Project,” paper SPE 63221 presented at the 2000 SPE Annual Technical Conference and Exhibition, Dallas, Texas, 1-4 October.

17. Guan, L. and Du, Y.: “Fast Method Finds Infill Drilling Potentials in Mature-Tight Reservoirs,” paper SPE 91755 presented at the 2004 SPE International Petroleum Conference, Puebla, Mexico, 8-9 November.

# VITA


| | |
|---|---|
| Name: | Ozgur Senel |
| Address: | Harold Vance Department of Petroleum Engineering<br>3116 TAMU<br>College Station, TX 77843-3116 |
| Education: | B.Sc., Petroleum and Natural Gas Engineering, Middle East Technical University |
| | M.Sc., Petroleum Engineering, Texas A&M University |